



EXPERIMENTAL AND THEORETICAL STUDIES ON MILD STEEL CORROSION INHIBITION BY THE GRIESEOFULVIN IN 1 M HCl

Dakeshwar Kumar Verma^[a], Fahmida Khan^[b], Chandrabhan Verma^[c], Rajendran Susai^[d,e] and M. A. Quraishi^[c]

Keywords: adsorption; mild steel; corrosion inhibitor; grieseofulvin

The inhibition effect of grieseofulvin against the mild steel corrosion in 1 M HCl solution has been investigated by potentiodynamic polarization measurements, electrochemical impedance spectroscopy (EIS) and quantum chemical methods. It was found that grieseofulvin acts as a good mild steel corrosion inhibitor in the acid solution at temperature ranging from 298-328 K. The potentiodynamic polarization study reveals that grieseofulvin acts as mixed type inhibitor. The adsorption of grieseofulvin on mild steel follows the Langmuir adsorption isotherm. Scanning electron microscopy equipped with energy dispersive spectroscopy (SEM-EDS) studies established that grieseofulvin formed a protective layer on the surface of mild steel.

* Corresponding Authors

Tel: +91-9307025126

Fax: +91-542-2368428

E-Mail: maquraishi.apc@itbhu.ac.in

- [a] Department of Chemistry, VEC Lakhapur, Sarguja University, Ambikapur, Chhattisgarh, India, 497116
 [b] Department of Chemistry, National Institute of Technology Raipur, Raipur, Chhattisgarh, India, 492010
 [c] Department of Applied Chemistry, Indian Institute of Technology, Banaras Hindu University, Varanasi-221005,
 [d] Servite College of Education for Women, Thogaimalai-621313, Tamil Nadu, India
 [e] Corrosion Research Centre, Post Graduate and Research Department of Chemistry, GTN Arts College, Dindigul-624005, India

Introduction

Mild steel corrosion inhibition is a matter of theoretical as well as practical importance which is an engineering material widely used in process industries, boilers, oil and gas, water pipelines, cooling water systems and refining and extraction etc. several acidic solutions are widely used in many industrial process such as acid cleaning, acid pickling, oil well acidizing and acid descaling.¹⁻³ These process generally leads to serious metallic corrosion. Use of an inhibitors is the sensible and most effective approach to protect the metal from corrosion.⁴ Electronic characteristics and molecular structure of inhibitors molecules are the main factors in establishing the adsorption capability of inhibitors on metal surfaces.⁵ The greater efficiency of these inhibitors is associated to the presence of various polar elements such as N, O, S and P in the organic molecules as well as pi electrons.⁶⁻⁸ The presence of such hetero atoms with lone pair(s) of electrons and π electrons in the molecular structure increase the adsorption ability of inhibitor molecules on the metal surface.⁹ The inhibitive effect of some antibacterial drugs namely cloxacillin, amoxicillin, ampicillin and flucloxacillin was studied. The corrosion inhibition mechanism of these drugs was attributed to blocking the metal surface by the formation of protective film.¹⁰

Nowadays, various experimental and theoretical techniques have been developed to study the structural properties of inhibitor molecules and their activity towards metal surfaces, but quantum chemical calculations based on density functional theory (DFT) have led to an attractive theoretical method because it gives several vital parameters. A quantum chemical approach is adequately sufficient to forecast the inhibitor effectiveness.

The aim of the present study is to investigate the mild steel corrosion behaviour in 1 M HCl in the presence and absence of antifungal drug namely, Grieseofulvin which is the commercial name of 7-chloro-2',4,6-trimethoxy-6'-methyl-3H,4'H-spiro[1-benzofuran-2,1'-cyclohex[2]ene]-3,4'-dione.¹¹ The present study is carried out using the weight loss measurements, DFT, Tafel polarization, and electrochemical impedance techniques. Protective film formation against acid attack on metal surface was confirmed by Scanning electron microscopy equipped with energy dispersive spectroscopy (SEM-EDS). The activation energy and thermodynamic parameters (ΔH^* and ΔS^*) of the inhibitor were investigated. Several commonly used adsorptions were also tested for their significance in defining the adsorption behaviour of the inhibitor. The chemical structure of the investigated inhibition is given in Fig.1.

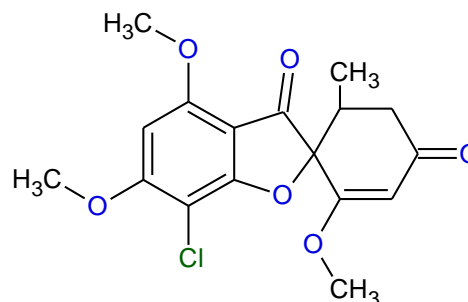


Figure 1. Molecular structure of grieseofulvin

Experimental

Materials preparation

Mild steel specimens having chemical composition (% wt): Fe (98.67), C (0.22), O (0.06), Mn (0.51), P (0.03), S (0.02) and Cr (0.49) were used for electrochemical, weight loss and surface measurements. Before performing the experiments, the metallic specimens were cleaned with the help of emery papers of different grades, washed with distilled water, degreased with acetone and stored in moisture free desiccators. The test solution of 1 M HCl was prepared by dilution of analytical grade HCl (Merck) with purified water obtained from Elix essential 10 millipore water purifier. During course of weight loss and electrochemical experiments, the concentration range of inhibitor was allowed to varied from 100-400 ppm.

Electrochemical measurements

Gamry Potentiostat/Galvanostat electrochemical workstation (ESA300 USA) with three electrode cell assembly was used for impedance measurements. In cell assembly, saturated calomel electrode (SCE) served as reference electrode, and a bare mild steel electrode and platinum electrode were used as working and counter electrodes, respectively. The working electrode with exposed area 1 cm² was kept in test solution for 30 minutes for attainment of steady open circuit potential (OCP) before electrochemical tests. The impedance measurements were performed in the frequency range from 100 kHz to 10 MHz with a.c. ± 10 mV and Nyquist plots were obtained. The potential range of ± 250 mV vs. corrosion potential at a scan rate of 1 mV s⁻¹ was applied for polarization experiment in the same cell assembly.

Weight loss measurements

Weight loss measurements were performed at temperature ranging from 298-328 K with different concentration of inhibitor at the immersion period of 6h. After the 6h of immersion time the mild steel strips were picked out, cleaned and dried. Electronic balance (METTLER TOLEDO sensitivity up to 0.0001gm) was used for weigh the mild steel specimens. The corrosion rate (C_R) in terms of weight loss was calculated according to equation (1):¹²

$$C_R = \frac{W}{At}$$

where

A is the total area of metal specimen in cm²,

W is the average weight loss in mg, and

t is the exposure time (6h).

The % inhibition efficiency ($\eta\%$) was calculated as given:¹²

$$\eta\% = \frac{C_R - C_{R(i)}}{C_R} \times 100 \quad (2)$$

where C_R and $C_{R(i)}$ are the corrosion rates of the test specimens without and with the inhibitor respectively.

Surface analysis

Scanning electron microscope and energy dispersion x-ray spectroscopy (SEM-EDS ZEISS EVO SEM 18 model 20mm Detector equipped with INCA 250 EDS X-MAX 20 Detector Oxford) were used to study the surface morphology and surface composition of mild steel in 1 M HCl in the presence and absence of inhibitor respectively.

Quantum chemical study

Gaussian 09 (G 09) software package is used for quantum chemical calculation of grieseofulvin with geometrically optimised structure.³² The backe's three parameters hybrid exchange functional and Lee-Yang-Parr non-local correlation function (B3LYP) as well as 3-21G basic set were employed for calculations. The theoretical parameters such as lowest unoccupied molecular orbital (LUMO) energies, highest occupied molecular orbital (HOMO) energies, energy gap ΔE ($E_{\text{HOMO}} - E_{\text{LUMO}}$) and dipole moment (μ) were calculated.

Result and discussion

Potentiodynamic polarization measurements

Potentiodynamic polarization curves for grieseofulvin in 1 M HCl solution with and without inhibitor at room temperature represented in Fig. 2.

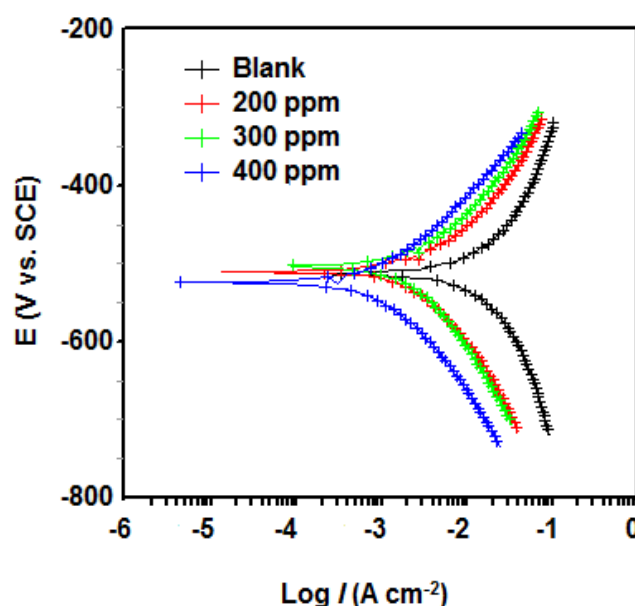


Fig. 2. Tafel polarization curves of mild steel in 1 M HCl with and without grieseofulvin.

Table 1. Potentiodynamic polarization parameters of mild steel in 1 M HCl at room temperature containing different concentration of grieseofulvin.

Conc., ppm	i_{corr} , mA/cm ²	E_{corr} , (mV/SCE)	β_a , (mV/dec)	β_c , (mV/dec)	ϑ	$\eta\%$
Blank	85.10	-514	665.2	1219	-	-
200	21.68	-511	109.3	193	0.745	74.52
300	14.31	-506	127.0	221.4	0.831	83.18
400	4.777	-525	108.6	129.2	0.943	94.38

Table 2. Impedance data of mild steel in 1 M HCl in the presence and absence of inhibitor at room temperature.

Conc., ppm	R_s , Ω cm ²	R_{ct} , Ω cm ²	C_{dl} , μ F cm ⁻²	ϑ	$\eta\%$
Blank	0.160	1.952	120.77	-	-
200	1.407	5.791	82.57	0.662	66.29
300	2.273	19.77	81.43	0.901	90.12
400	1.194	25.27	68.19	0.922	92.22

Important kinetic parameters including corrosion potential (E_{corr}), corrosion current density (i_{corr}), and percentage inhibition efficiency ($\eta\%$) from Tafel plots were calculated and given in Table 1. The inhibition efficiency was calculated from the values of corrosion current density (i_{corr}) which itself derived by extrapolating the linear segments of anodic and cathodic Tafel slopes, using the following relation:¹³

$$\eta\% = \frac{i_{corr}^0 - i_{corr}^i}{i_{corr}^0} \times 100 \quad (3)$$

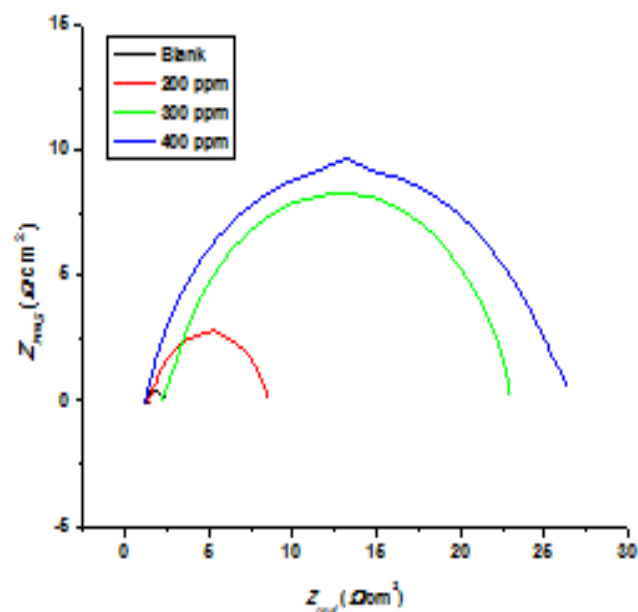
where i_{corr} and i_{corr}^i are the corrosion current densities without and with inhibitor, respectively.

Table 1 shown that corrosion current density (i_{corr}) of cathodic and anodic curves decreases and inhibition efficiency increases as the inhibitor concentration increases in compared to blank 1 M HCl solution. The decrease in corrosion current density and increased inhibition efficiency suggests the adsorption of grieseofulvin molecules on the mild steel surface at the metal/solution interface. Adsorption of inhibitor molecules mitigates the corrosion process by forming the protective layer on the mild steel surface where direct corrosive attack occurs.¹⁴ From the results depicted in Table 1 it can be seen that presence of inhibitor did not causes any significant change in the value of corrosion potential (E_{corr}) suggesting that investigated inhibitor behaves as mixed type.

Electrochemical impedance spectroscopy (EIS)

EIS analysis is an important and complementary tool undertaken for the determination of corrosion rates. Nyquist and bode plots were represented in Figs. 3 and 4 with and without the inhibitor at temperature 298 K. It is concluded from Nyquist plots (Fig. 3) shows that the curves approximated by a single capacitive depressed semi-circles.

This displaying that the corrosion process in mild steel is controlled by charge transfer process.¹⁵ Also, these impedance diagrams are not perfect, this features is related to inhomogeneity and frequency dispersion of metal as a result of surface roughness.¹⁶ Fig. 5 represents the equivalent circuit model which is used to explain the impedance spectra for Nyquist plots in steel/acid solution interface.¹⁷ In this equivalent circuit modal, R_{ct} is charge transfer resistance, R_s is the solution resistance and CPE is a constant phase element. A constant phase element (CPE) is used instead of double layer capacitance (C_{dl}) for the description of a frequency phase shift between an applied potential and its current response. The double layer capacitance was replaced by the constant phase element (CPE), in order to obtain the representative fit.

**Figure 3.** Nyquist plot for mild steel in 1 M HCl solution at different concentrations of inhibitor at 298 K.

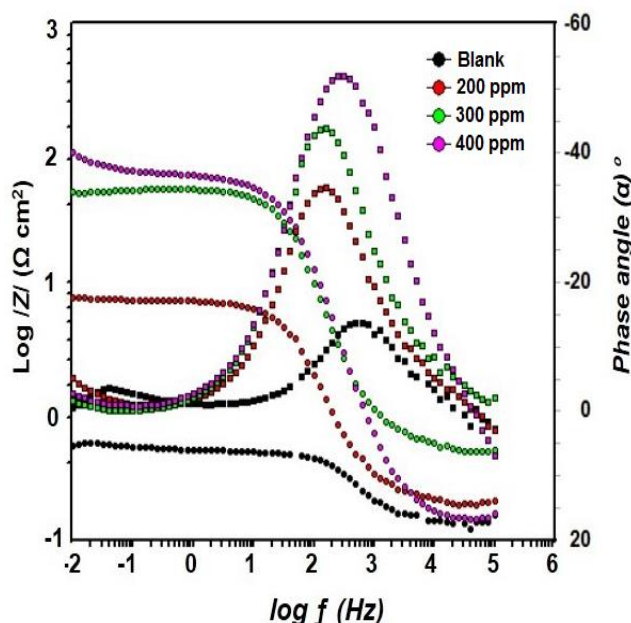


Figure 4. Bode plots of impedance spectra for mild steel in 1 M HCl solution with and without the inhibitor at 298 K.

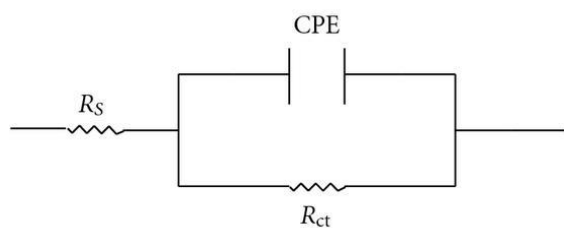


Figure 5. Equivalent circuit model used to fit the impedance spectra.

The double layer capacitance (C_{dl}) is defined by the mathematical expression.¹⁸

$$C_{dl} = Y_0 (\omega_{max})^{n-1} \quad (4)$$

where

n is CPE exponent (phase shift),

Y_0 is CPE coefficient,

ω is the angular frequency and

ω_{max} shows the frequency at which the imaginary component reaches the maximum.

Value of n can be associated with non-uniform current distribution, a distribution of reaction rates and roughness of electrode surface etc.¹⁹ Depending on the value of n , CPE can represent capacitance ($n = 1$, $Y_0 = C$), represent resistance ($n = 0$, $Y_0 = R$), Warburg impedance ($n = 0.5$, $Y_0 = W$) or inductance ($n = -1$, $Y_0 = L$). Various electrochemical impedance parameters such as CPE, R_{ct} , R_s , and n calculated using the nyquist plot. By using charge transfer resistance (R_{ct}) values the $\% \eta$ were calculated following the equation below.²⁰

$$\% \eta = \frac{R_{ct(inh)} - R_{ct}}{R_{ct(inh)}} \times 100 \quad (5)$$

where $R_{ct(inh)}$ and R_{ct} are the charge transfer resistances with and without inhibitor respectively. Corresponding values of EIS measurements shown in Table 2. It is clear from Table 2 that grieseofulvin exhibits the highest inhibition efficiency of 92.22 % at the 400 ppm concentration of inhibitor.

Weight loss measurements

Various corrosion parameters such as corrosion rate (ρ), inhibition efficiency ($\% IE$) and surface coverage (θ) were determined from gravimetric analysis data for mild steel in 1 M HCl solution with and without inhibitor of different concentrations (100-400 ppm). For the mild steel, the mean value of corrosion rate ($\text{mg cm}^{-2} \text{h}^{-1}$) was determined for every concentration and inhibition efficiency was calculated using equations (1) and (2) respectively. Measurement performed in temperature ranging from 298-328 K after 6h of immersion period. The variation of corrosion rates and inhibition efficiency with temperature and inhibitor concentration for grieseofulvin is listed in Table 3. From Table 3 it is observed that grieseofulvin exhibits its higher inhibition efficiency (94.35 %) at optimum concentration (400 ppm) of inhibitor. Better inhibition efficiency at optimum concentration of grieseofulvin may be attributed to more coverage of mild steel by inhibitor molecules.²¹ Based on the above result grieseofulvin can be considered as a good corrosion inhibitor for mild steel in 1 M HCl solution.

Adsorption and thermodynamic consideration

The efficiency of inhibitor molecules as corrosion inhibitor can be considered as the adsorption of these molecules on the mild steel surface through their hetero polar atoms viz. P, O, N and S.²² The experimental data have been tested with several adsorption isotherms namely Langmuir, Frumkin and Temkin to obtain information regarding the type and mode of adsorption of grieseofulvin. In present study the Langmuir adsorption isotherm fitted well and the isotherm is expressed by the mathematical equation given below:²³

$$\frac{C}{\theta} = \frac{1}{K_{ads}} + C \quad (6)$$

where

θ is the surface coverage,

C is the inhibitor concentration in electrolyte and

K_{ads} is equilibrium constant of the adsorption process which is related to the Gibbs energy of adsorption (ΔG_{ads}) according to given equation.²³

$$\Delta G_{ads} = -RT \ln (55.5 K_{ads}) \quad (7)$$

Table 3. Various corrosion parameters obtained from weight loss measurements for mild steel in 1 M HCl with and without inhibitor at studied temperatures.

Temperature, K	Concentration, ppm	C_R , mgcm ⁻² h ⁻¹	($\eta\%$)	θ
298	0.0	0.984	-	-
	100	0.146	85.16	0.851
	200	0.119	87.90	0.879
	300	0.097	90.14	0.901
	400	0.075	92.37	0.923
308	0.0	1.931	-	-
	100	0.183	90.52	0.905
	200	0.161	91.66	0.916
	300	0.147	92.38	0.923
	400	0.109	94.35	0.943
318	0.0	3.998	-	-
	100	0.689	82.76	0.827
	200	0.463	88.41	0.884
	300	0.409	89.76	0.897
	400	0.327	91.82	0.918
328	0.0	5.497	-	-
	100	1.189	78.37	0.783
	200	1.022	81.40	0.814
	300	0.810	85.26	0.852
	400	0.687	87.50	0.875

where

T is the thermodynamic temperature,

K is the binding constant and

R is gas constant.

Fig. 6 represents the relationship between C/θ and inhibitor concentration (C_{inh}) which represents typical Langmuir adsorption isotherm. A very good linear plot was observed with regression coefficient up to 0.999 and slope of unity. The value of K_{ads} value can be calculated from the intercept of straight line and average values of K_{ads} -21.67 kJ mol⁻¹ was obtained and are given in Table 4. The higher negative values of ΔG_{ads} suggests the spontaneity of the stability of the adsorbed film and adsorption process on the mild steel surface,²⁴ as well as strong interaction.

Effect of temperatures

Temperature has a great effect on the mild steel electrochemical corrosion rate in 1 M HCl. Many changes such as decomposition of the inhibitor, desorption of inhibitor and rapid etching may occur on the metal surface in different temperatures in the inhibitor solution. In case of metal corrosion in 1 M HCl solution, the rate of corrosion increases exponentially with temperature increases because the hydrogen evolution overpotential decreases.²⁵ Apparent activation energy (E_a), can be calculated from the values of corrosion rate obtained from weight loss measurement and applying the Arrhenius equation.²⁶

$$C_R = A \exp\left(\frac{-E_a}{RT}\right) \quad (8)$$

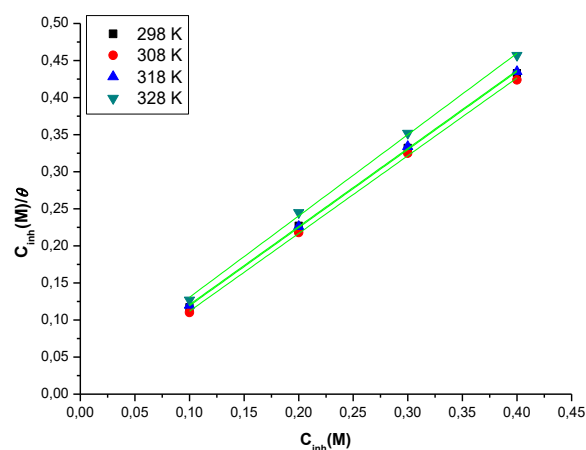


Figure 6. Langmuir adsorption linear fitting curves for mild steel in 1 M HCl at different temperatures and concentrations of inhibitor.

where

C_R is the corrosion rate,

E_a is the activation energy,

A is the frequency factor,

R is the gas constant (8.314 J K⁻¹ mol⁻¹) and

T is the absolute temperature.

The slope of $\log \rho$ versus $1/T$ K⁻¹ (K) plots for mild steel with and without inhibitor is presented in Fig. 7 and corresponding parameters were given in Table 5. Usually E_a values with inhibitor (100-400 ppm) are higher than that of without inhibitor. These increased values of E_a indicating a strong inhibitive action of grieseofulvin by increasing the energy barrier for the metal corrosion process.²⁷

The enthalpy of activation (ΔH^*) and entropy of activation (ΔS^*) in 1 M HCl solution for the mild steel corrosion were obtained by applying the transition-state equation:¹²

$$C_R = \frac{RT}{Nh} \exp\left(\frac{\Delta S_a}{R}\right) \exp\left(-\frac{H_a}{RT}\right) \quad (9)$$

where

ΔH^* is the enthalpy of activation,

ΔS^* is the entropy of activation,

ρ is the corrosion rate,

h is plank's constant (6.626176×10^{-34}),

R is gas constant and

N is the Avogadro's number.

Fig. 8 represents the linear plot of $\log \rho/T$ vs. $1/T \text{ K}^{-1}$ gave an intercept of $\log(R/Nh) + (\Delta S^*/2.303)$ and a straight line with a slope of $\Delta H^*/2.303R$. The values of ΔH^* and ΔS^* were calculated and summarised in Table 5.

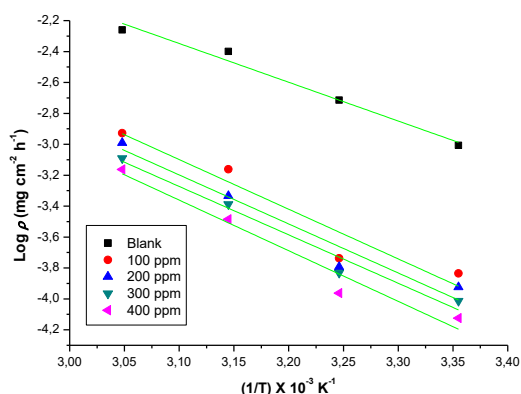


Figure 7. Arrhenius plots for the mild steel corrosion in 1 M hydrochloric solution in the presence and absence of inhibitor at studied temperatures.

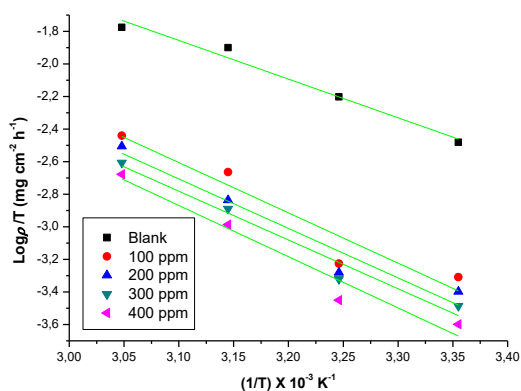


Figure 8. Transition state plots of $\text{Log } C_R(\rho)/T$ vs. $1/T$ in the presence and absence of inhibitor for mild steel corrosion in 1 M HCl solution.

The enthalpy of activation ΔH^* showed similar trend like the apparent activation energy values i.e. values increases as inhibitor concentration increases. The entropy of activation energy ΔS^* values is more negative in the absence of inhibitor than the presence of inhibitor, indicates the activated complex is more ordered in uninhibited solution. The less negative values of ΔS^* suggest the driving force for the adsorption process on metal/solution interface.²⁸

Surface (SEM-EDX) analyses

The formation of protective layer by inhibitor and elements present on the mild steel surface were confirmed by SEM and EDX analysis. These analyses were performed before and after the exposure to the acidic solution in the absence and presence of inhibitor and represented in Figs. 9 and 10 respectively.

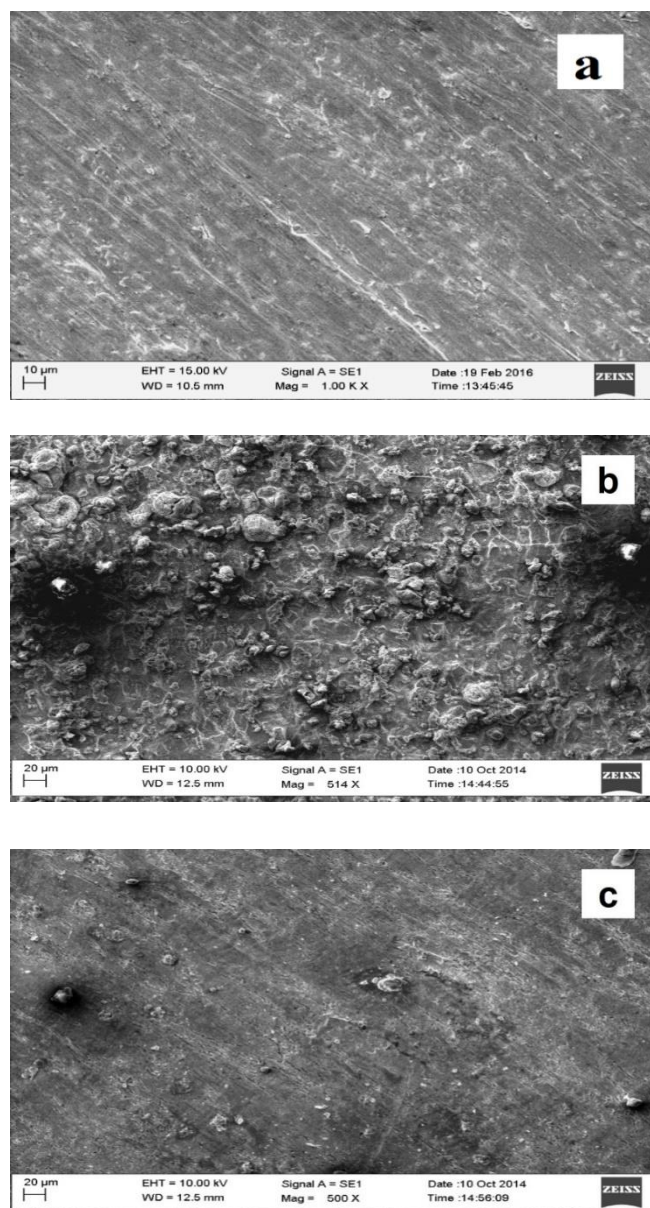


Figure 9. SEM microphotographs of the mild steel surface: (a) polished metal surface, (b) metal immersed in 1 M HCl solution without and (c) with the inhibitor.

Table 4. Langmuir parameters for the adsorption of grieseofulvin on the mild steel surface in 1 M HCl solution.

T (K)	R ²	Slope	K _{ads} , L mol ⁻¹	ΔG _{ads} , kJ mol ⁻¹
298	0.999	1.053	71.42	-20.52
308	0.999	1.049	142.8	-22.99
318	0.999	1.053	66.66	-21.72
328	0.998	1.097	47.61	-21.48

Table 5. Activation parameters mild steel dissolution in 1 M HCl with and without the inhibitor at studied temperatures.

Conc., ppm	A, mg cm ⁻² h ⁻¹	E _a , kJ mol ⁻¹	ΔH*, kJ mol ⁻¹	ΔS*, kJ mol ⁻¹
0.0	2.65 × 10 ⁵	48.00	45.45	-11.08
100	7.26 × 10 ⁶	61.50	58.97	-07.72
200	4.30 × 10 ⁶	60.71	58.14	-08.30
300	2.69 × 10 ⁶	59.93	57.32	-08.79
400	6.15 × 10 ⁶	62.68	60.19	-07.92

Table 6. Percentage elemental contents (wt %) recorded from EDX spectra of mild steel in the absence and presence (400 ppm) of grieseofulvin in 1 M HCl.

Medium	Composition (wt %)							
	Fe	C	O	P	S	Cr	Mn	Cl
Mild steel (MS)	98.24	0.213	0.106	0.048	0.512	0.481	0.392	-
MS in 1 M HCl	89.13	1.422	3.698	0.029	0.312	0.325	0.289	4.786
MS in grieseofulvin	93.55	2.159	2.361	0.025	0.119	0.311	0.254	1.211

Table 7. Quantum chemical parameters for the grieseofulvin

Inhibitor	E _{HOMO} , eV	E _{LUMO} , eV	ΔE, eV	μ, eV	γ
Grieseofulvin	-0.0423	-0.0059	0.0364	3.2396	0.0182

Figure 9a represents the surface morphology of polished mild steel coupon exhibit smooth and homogeneous surface. Whereas Fig. 9b and 9c reveals the mild steel samples in the absence and presence of inhibitor respectively.

Specimen in the uninhibited solution is highly damaged due to direct acid attack (Fig. 9b) and mild steel surface is not as damaged as in the case of uninhibited acidic solution shown in Fig. 9c. This reveals the protective layer formation of inhibitor on mild steel surface thus protecting it from direct corrosive attack.²⁹

EDX analysis was performed in order to get information regarding the elemental composition of mild steel surface in the presence and absence of grieseofulvin in 1 M HCl solution. The EDX spectra and corresponding values of elementals composition (wt%) shown in Fig. 10 and Table 6 respectively. The EDX data in Table 6 shows that the mild steel surface in the absence of inhibitor show a higher chloride content of due to corrosive attack of hydrochloric acid (Fig. 10b) whereas metal in inhibited solution shows the lower chloride content of (Fig. 10c). SEM-EDS analysis further confirm the adsorption of grieseofulvin molecules on the mild steel surface and decrease the corrosion rate.³⁰

Quantum chemical analysis

Quantum chemical calculations were performed in order to study the molecular structure of grieseofulvin on the inhibition efficiency by using density functional theory (DFT). Various electronic properties such as the energy of lowest unoccupied molecular orbital (ELUMO), energy of highest occupied molecular orbital (EHOMO), and energy gap (ΔE) between the LUMO and HOMO, global hardness (γ), softness (σ), and dipole moment (μ) were determined by optimizing the structure. The optimized structure, lowest unoccupied molecular orbital (LUMO) and highest occupied molecular orbital (HOMO) of grieseofulvin are shown in Fig.11 (a, b & c).

Corresponding values of parameters are given in Table 7. For the calculation of global hardness (γ) the equation used is given as:³¹

$$\gamma = \frac{E_{LUMO} - E_{HOMO}}{2} \quad (10)$$

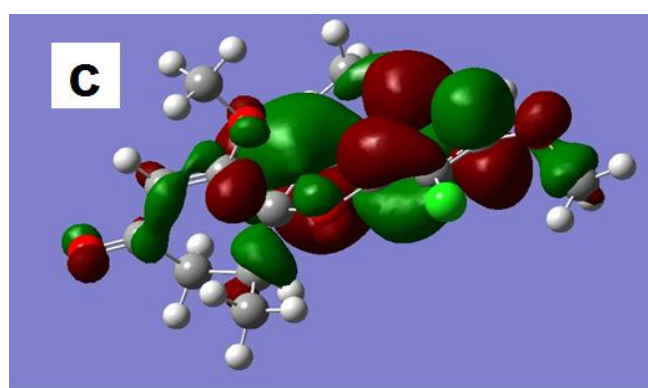
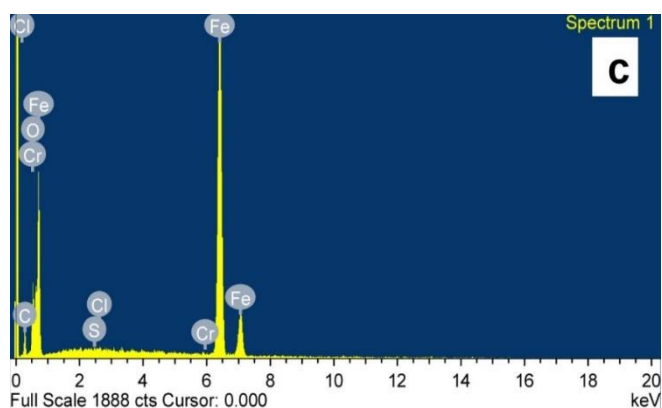
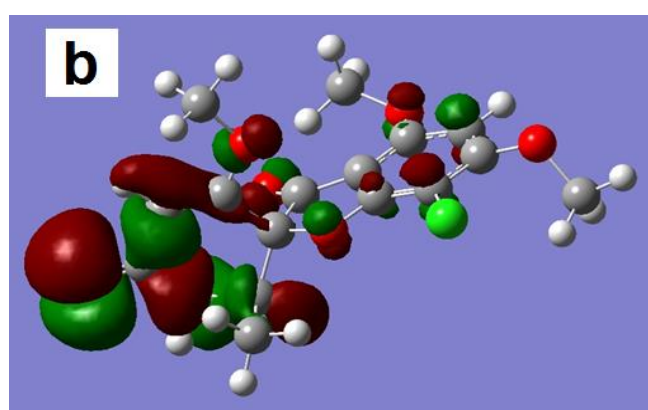
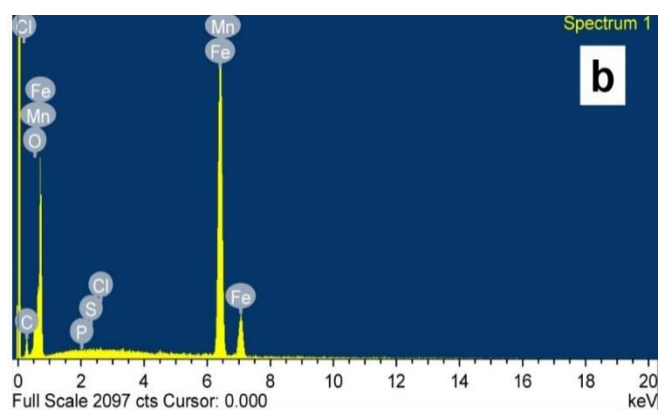
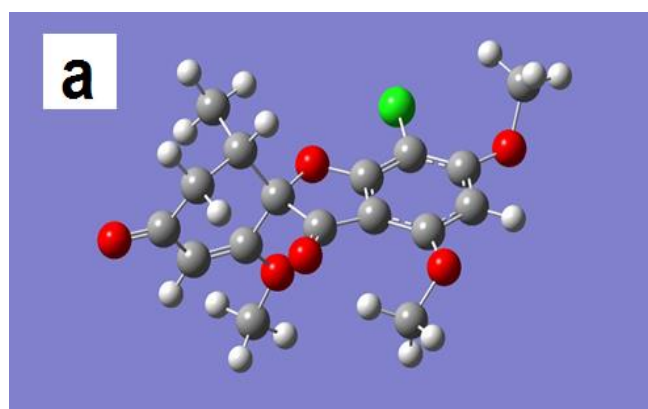
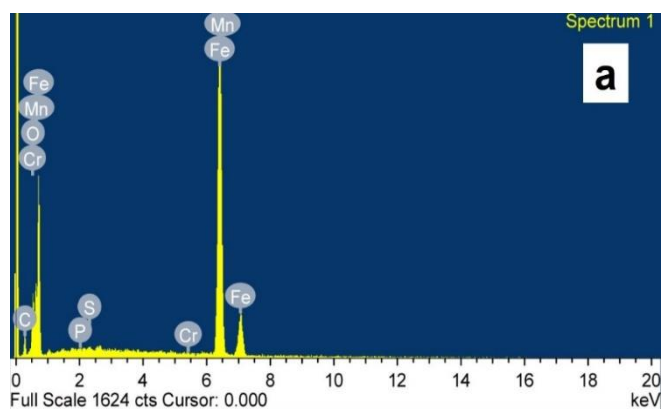


Figure 10. EDX spectra of (a) polished mild steel surface, (b) mild steel immersed in 1 M HCl and (c) mild steel in the inhibited solution.

Figure 11. (a) The optimized structure, (b) LUMO and (c) HOMO for the grieseofulvin.

The calculated frontier molecular orbital (FMO) properties for grieseofulvin is given in Table 7. Higher value of E_{HOMO} of molecule indicates the higher electron donating ability of inhibiting molecule to appropriate acceptor molecules. Consequently, an increased E_{HOMO} value reveal good adsorption ability of inhibitor on the metal surface. Lower E_{LUMO} value of molecule measures its greater ability to accept the electrons.³³

Conclusion

Grieseofulvin exhibits good anticorrosive property towards the mild steel in 1 M HCl solution at studied temperatures (298-328K). Potentiodynamic polarization measurements reveals the mixed type inhibition property of grieseofulvin. Impedance analysis shows that grieseofulvin reducing the rate of charge transfer process by forming

protective layer on the mild steel surface. Weight loss measurements exhibits the increased inhibition efficiency (IE%) with increasing inhibitor concentration and the maximum IE% was found to be 94.35 at 400 ppm inhibitor concentration. The adsorption of the inhibitor obeys the Langmuir adsorption isotherm at studied temperatures. The values of free energy of adsorption shows that the spontaneous adsorption process of inhibitor on mild steel surface. SEM-EDX analysis also show that inhibitor molecules inhibits the mild steel corrosion by formation of protective layer on mild steel surface. The results of quantum chemical analysis revealed good correlation with the studied experimental results.

References

- Shukla, S. K., Quraishi, M. A., Ceftriaxone: a novel corrosion inhibitor for mild steel in hydrochloric acid, *J. Appl. Electrochem.*, **2009**, *39*, 1517-1523. <https://doi.org/10.1007/s10800-009-9834-1>
- Gobara, M., Baraka, A., Zaghloul, B., Inhibition of mild steel corrosion in sulphuric acid solution using collagen, *Res. Chem. Intermed.*, **2014**, doi: 10.1007/s11164-014-1809-0. <https://doi.org/10.1007/s11164-014-1809-0>
- Pavithra, M. K., Venkatesha, T. V., Kumar M. K. P., Manjunatha, K., Investigation of the inhibition effect of ibuprofen triazole against mild steel corrosion in an acidic environment, *Res. Chem. Intermed.*, **2014**, <https://doi.org/10.1007/s11164-014-1804-5>.
- Saha, S.K., Dutta, A., Ghosh, P., Sukul, D., Banerjee, P., Adsorption and corrosion inhibition effect of Schiff base molecules on the mild steel surface in 1 M HCl medium: a combined experimental and theoretical approach, *Phys. Chem. Chem. Phys.*, **2015**, *17*, 5679-5690. <https://doi.org/10.1039/C4CP05614K>, PMID:25623363
- Fiori-Bimbi, M. V., Alvarez, P. E., Vaca H., Gervasi, C. A., corrosion inhibition of mild steel in HCl solution by pectin, *Corros. Sci.*, **2015**, *92*, 192-199. <https://doi.org/10.1016/j.corsci.2014.12.002>
- Singh, P., Singh, D. P., Tiwari, K., Mishra, M., Singh, A. K., V. P. Singh, Synthesis, structural investigation and corrosion inhibition studies on Mn(II), Co (II), Cu (II) and Zn (II) complex with 2-amino-benzoic acid (phenyl-pyridin-2-yl-methylene)-hydrazide, *RSC Adv.*, **2015**, *5*, 45217-45230. <https://doi.org/10.1039/C4RA11929K>
- Bai, L., Feng, L., Wang, H. Y., Lu Y. B., Lei, X. W., Bai, F. L., comparison of the synergistic effect of counterions on the inhibition of mild steel corrosion in acid solution: electrochemical, gravimetric and thermodynamic studies, *RSC Adv.*, **2015**, *5*, 4716-4726. <https://doi.org/10.1016/j.electacta.2015.10.100>
- Souza, F. S. D., Spinelli, A., Caffeic acid as a green corrosion inhibitor for mild steel, *Corros. Sci.*, **2009**, *51*, 642-649. <https://doi.org/10.1016/j.corsci.2008.12.013>
- Solmazm, R., Investigation of corrosion inhibition mechanism and stability of vitamin B1 on mild steel in 0.5 M HCl solution, *Corros. Sci.*, **2014**, *81*, 75-84. <https://doi.org/10.1016/j.corsci.2013.12.006>
- Abdallah, M., Antibacterial drugs as corrosion inhibitors for corrosion of aluminium in hydrochloric solution, *Corros. Sci.*, **2004**, *46*, 1981-1996. <https://doi.org/10.1016/j.corsci.2003.09.031>
- Stuart, M. C., Kouimtzis, M., Hill, S. R., WHO model formulary, **2008**, p.no. 149.
- Verma, D. K., Khan, F., Corrosion inhibition of mild steel in hydrochloric acid using extract of glycine max leaves, *Res. Chem. Intermed.*, **2016**, *42*, 3489-3506. <https://doi.org/10.1007/s11164-015-2227-7>
- Sudheer, Quraishi, M. A., The corrosion inhibition effect of aryl pyrazolo pyridines on copper in hydrochloric acid system: computational and electrochemical studies, *RSC Adv.*, **2015**, *5*, 41923-41933. <https://doi.org/10.1039/C5RA03966E>
- Alkhathlan, H. Z., Khan, M., Abdullah, M. M. S., Aimayouf, A. M., Ahmed, A. Y. B. H., Alothman, Z. A., Mousa, A. A., Anticorrosive assay-guided isolation of active phytoconstituents from *Anthemis pseudocotula* extract and a detailed study of their effect on the corrosion of mild steel in acidic media, *RSC Adv.*, **2015**, *5*, 54283-54292. <https://doi.org/10.1039/C5RA09154C>
- Ostovari, A., Hoseinie, S. M., Peikari, M., Shadzadeh, S. R., Hashemi, S. J., Corrosion inhibition of mild steel in 1 M HCl solution by henna extract: A comparative study of the inhibition by henna and its constituents (Lawson, Gallic acid, a-D-Glucose and Tannic acid), *Corros. Sci.*, **2009**, *51*, 1935-1949. <https://doi.org/10.1016/j.corsci.2009.05.024>
- Li, X. H., Deng, S., Fu, H., Inhibition by *Jasminum nudiflorum* Lindl. leaves extract of the corrosion of cold rolled steel in hydrochloric acid solution, *J. Appl. Electrochem.*, **2010**, *40*, 1641-1649. <https://doi.org/10.1007/s10800-010-0151-5>
- Quraishi, M.A., Singh, A., Singh, V. K., Yadav, D. K., Singh, A. K., Green approach to corrosion inhibition of mild steel in hydrochloric acid and sulphuric acid solutions by the extract of *Murraya koenigii* leaves, *Mater. Chem. Phys.*, **2010**, *122*, 114-122. <http://dx.doi.org/10.1016/j.matchemphys.2010.02.066>
- Shahi, G., Verma, C. B., Ebenso, E. E., Quraishi, M. A., Thermodynamic and Electrochemical investigation of (9-[(R) 2[[bis [(isopropoxycarbonyl)oxy]methoxy] phosphinyl] methoxy] propyl] adenine fumarate) as Green Corrosion Inhibitor for Mild Steel in 1M HCl, *Int. J. Electrochem. Sci.*, **2015**, *10*, 1102 - 1116.
- Soltani, N., Tavakkoli, N., Khayatkashani, M., Jalali, M. R., Mosavizade, A., Green approach to corrosion inhibition of 304 stainless steel in hydrochloric acid solution by the extract of *Salvia officinalis* leaves, *Corros. Sci.*, **2012**, *62*, 122-135. <https://doi.org/10.1016/j.corsci.2012.05.003>
- Korde, R., Verma, C. B., Ebenso, E.E., Quraishi, M.A., Electrochemical and Thermo Dynamical Investigation of 5-ethyl 4-(4-methoxyphenyl)-6-methyl-2-thioxo-1, 2, 3, 4 tetrahydropyrimidine-5-carboxylate on Corrosion Inhibition Behavior of Aluminium in 1M Hydrochloric Acid Medium, *Int. J. Electrochem. Sci.*, **2015**, *10*, 1081 - 1093.
- Singh, A. K., Khan, S., Singh, A., Quraishi, S. M., Quraishi, M. A., Ebenso, E. E., Inhibitive effect of chloroquine towards corrosion of mild steel in hydrochloric acid solution, *Res. Chem. Intermed.*, **2013**, *39*, 1191-1208. <https://doi.org/10.1007/s11164-012-0677-8>
- Khadraoui, A., Khelifa, A., Hamitouche, H., Mehdaoui, R., Inhibitive effect by extract of *Mentha rotundifolia* leaves on the corrosion of steel in 1 M HCl solution, *Res. Chem. Intermed.*, **2014**, *40*, 961-972. <https://doi.org/10.1007/s11164-012-1014-y>
- Verma, D. K., Khan, F., Green approach to corrosion inhibition of mild steel in hydrochloric acid medium using extract of spirogyra algae, *Green chem lett rev.*, **2016**, *9(1)*, 52-60. <https://doi.org/10.1080/17518253.2015.1137976>
- Nazeer, A. A., Shalabi, K., Fouda, A. S., Corrosion inhibition of carbon steel by Roselle extract in

- hydrochloric acid solution: electrochemical and surface study, *Res. Chem. Intermed.*, **2014**, DOI 10.1007/s11164-014-1570-4. <https://doi.org/10.1007/s11164-014-1570-4>
- ²⁵Hussin, M. H., Kassim, M. J., Inhibitive properties, thermodynamic and quantum chemical studies of alloxazine on mild steel corrosion in H₂SO₄, *Corros. Sci.*, **2011**, *53*, 263–275. <https://doi.org/10.1016/j.corsci.2010.09.020>
- ²⁶Obi-Egbedi, N.O., Obot, I.B., Inhibitive properties, thermodynamic and quantum chemical studies of alloxazine on mild steel corrosion in H₂SO₄, *Corros. Sci.*, **2011**, *53*, 263–275.
- ²⁷Noor, E. A., Al-Moubaraki, A. H., Thermodynamic study of metal corrosion and inhibitor adsorption processes in mild steel/1-methyl-4[(-X)-styryl pyridinium iodides/hydrochloric acid systems, *Mater. Chem. Phys.*, **2008**, *110*:145–154.
- ²⁸Vishwakarma, S., Mourya, P., Chaubey, N., Kumar, S., Singh, V. K., Singh, M. M., Strychnos nuxvomica, Piper longum and Mucuna pruriens seed extracts as eco-friendly corrosion inhibitors for copper in nitric acid, *RSC Adv.*, **2016**, <https://doi.org/10.1039/C6RA16481A>
- ²⁹Ramaganathan, B., Gopiraman, M., Olasunkanmi, L. O., Kabanda, M. M., Yesudass, S., Bahadur, I., Adekunle, A. S., Obote, I. B., Ebenso, E. E., Synthesized photo-cross-linking chalcones as novel corrosion inhibitors for mild steel in acidic medium: experimental, quantum chemical and Monte Carlo simulation studies, *RSC Adv.*, **2015**, *5*, 76675–76688. <https://doi.org/10.1039/C5RA12097G>
- ³⁰Tamilarasan, R., Sreekanth, A., Spectroscopic and DFT investigations on the corrosion inhibition behavior of tris(5-methyl-2-thioxo-1,3,4-thiadiazole)borate on high carbon steel and aluminium in HCl media, *RSC Adv.*, **2013**, *3*, 23681–23691. <https://doi.org/10.1039/c3ra43681k>
- ³¹Yadav, M., Sinha, R. R., Kumar, S., Sarkar, T. K., Corrosion inhibition effect of spiropyrimidinethiones on mild steel in 15% HCl solution: insight from electrochemical and quantum studies, *RSC Adv.*, **2015**, *5*, 70832–70848. <https://doi.org/10.1039/C5RA14406J>
- ³²Gaussian 09, Revision A.02, M. J. Frisch, G. W. Trucks, H. B. Schlegel, G. E. Scuseria, M. A. Robb, J. R. Cheeseman, G. Scalmani, V. Barone, B. Mennucci, G. A. Petersson, H. Nakatsuji, M. Caricato, X. Li, H. P. Hratchian, A. F. Izmaylov, J. Bloino, G. Zheng, J. L. Sonnenberg, M. Hada, M. Ehara, K. Toyota, R. Fukuda, J. Hasegawa, M. Ishida, T. Nakajima, Y. Honda, O. Kitao, H. Nakai, T. Vreven, J. A. Montgomery, Jr., J. E. Peralta, F. Ogliaro, M. Bearpark, J. J. Heyd, E. Brothers, K. N. Kudin, V. N. Staroverov, R. Kobayashi, J. Normand, K. Raghavachari, A. Rendell, J. C. Burant, S. S. Iyengar, J. Tomasi, M. Cossi, N. Rega, J. M. Millam, M. Klene, J. E. Knox, J. B. Cross, V. Bakken, C. Adamo, J. Jaramillo, R. Gomperts, R. E. Stratmann, O. Yazyev, A. J. Austin, R. Cammi, C. Pomelli, J. W. Ochterski, R. L. Martin, K. Morokuma, V. G. Zakrzewski, G. A. Voth, P. Salvador, J. J. Dannenberg, S. Dapprich, A. D. Daniels, O. Farkas, J. B. Foresman, J. V. Ortiz, J. Cioslowski, and D. J. Fox, Gaussian, Inc., Wallingford CT, 2009.
- ³³Soltani, N., Behpour, M., Oguzie, E. E., Mahluji, M., Ghasemzadeh, M. A., Pyrimidine-2-thione derivatives as corrosion inhibitors for mild steel in acidic environments, *RSC Adv.*, **2015**, *5*, 11145–11162. <https://doi.org/10.1039/C4RA11642A>

Received: 02.02.2017.

Accepted: 25.02.2017.